A minimal cage of a diamond twin with chirality

Toshiya M. Fukunaga[a], Takahide Kato[a], Koki Ikemoto[a,1], and Hiroyuki Isobe[a,1]

[a]Department of Chemistry, The University of Tokyo, Tokyo 113-0033, Japan

Edited by Jonathan Sessler, Department of Chemistry, The University of Texas at Austin, Austin, TX; received November 4, 2021; accepted January 5, 2022

A network of tetrahedral vertices can fill three-dimensional (3D) spaces in a beautiful and isotropic manner, which is found as diamonds with sp^3-hybridized carbon atoms. Although a network of trigonal vertices (i.e., another form of carbon atoms with sp^2-hybridization) naturally results in a lower-dimensional two-dimensional network of graphenes, an isotropic 3D arrangement of trigonal vertices has been of theoretical and mathematical interest, which has materialized as a proposal of a "diamond twin." We herein report the synthesis and optical resolution of a minimal cage of a chiral diamond-twin network. With triangular phenine units at 14 vertices, triply fused decagonal rings were assembled by forming 15 biaryl edges via coupling. A unique chirality of the network has been disclosed with the minimal cage, which may stimulate explorations of chiral carbonaceous materials.

diamond twin | carbon | chirality | helicity | stereoisomerism

The hybridization of carbon atoms plays an important role in determining the structures of their networks because the intrinsic geometries of sp^3-, sp^2-, and sp-carbon atoms dramatically alter the shapes of their tetrahedral (three-dimensional [3D]), trigonal (two-dimensional), and linear (one-dimensional) forms. A four-hand, tetravalent hybridization of sp^3-carbon is fascinating to not only lay people but also scientists through the beauty of diamonds, which has led chemists to explore segmental cages of diamondoids with adamantane as the minimal carbonaceous cage (1, 2). Recently, the beauty of 3D networks of sp^3-carbon atoms in diamonds has also been captured by mathematics adopting algebraic topology (3). Thus, the diamond crystal has been defined as a maximal abelian covering graph (MACG) of a quotient graph **1** (Fig. 1), which clarifies the presence of the strongly isotropic network of vertices (*A*, *B*) and edges (*a*–*d*) (4). This mathematical approach [i.e., topological crystallography (5)] has led to the rediscovery of a hypothetical diamond twin that is hereafter described as pollux in this work, after the younger brother in the Gemini twins. Indeed, the pollux has long attracted theoretical interest (6–8) and is mathematically redefined as a diamond twin due to its strong isotropy with maximal symmetry (3) (*SI Appendix*). Thus, pollux is an MACG of quotient graph **2** and shares topological beauty with diamond by achieving the maximal symmetry in filling 3D spaces (Fig. 1). In place of the four-hand vertices of diamond, pollux adopts three-hand, trivalent vertices of sp^2-carbon atoms; by linking four types of vertices (*A*–*D*) with six types of edges (*a*–*f*), the 3D spaces are filled in a strongly isotropic manner. Notably, unlike other isotropic carbonaceous networks of diamond or graphene, the isotropic pollux network gives rise to chirality, and two enantiomeric forms have been predicted. However, although this mathematical proposal is intriguing, the existence of pollux has been naturally questioned due to the highly strained, twisted orientations of connected sp^2-carbon atoms (6, 9, 10). Actually, when we examined a minimal cage segment of pollux, herein named polluxene, by density functional theory (DFT) calculations at the B3LYP/6-31G(d,p) level, it was not located as a stable molecule and collapsed into ring-closed [4.4.4]propellahexaene (Fig. 1) (11). Nonetheless, we realized that by preassembling six sp^2-carbon atoms in the form of 1,3,5-trisubstituted benzene (phenine) (12), a homothetic polluxene cage composed of sp^2-carbon atoms could be rationally designed. By using phenine as the trivalent, trigonal planar units, the minimal carbonaceous cage of pollux was thus realized in the form of phenine polluxene to cover all fundamental vertices and edges of quotient graph **2** in 3D space with a fused decagonal cage (Fig. 1). The synthesis of phenine polluxene allowed us to deliberate the structures and chirality of the pollux network, which clarified the presence of unique helical chirality. The chirality and stereoisomerism of pollux thus give us intriguing targets to exploit for the development of chiral carbonaceous materials (13).

Results and Discussion

Synthesis. The trivalent vertices of phenine units need to be linked to form triply fused decagonal macrocycles to form the minimal carbonaceous cage of pollux (3). For the synthesis of this unique decagonal cage, a stepwise ring-closing route was developed after unsuccessful trials of bisectional routes (Fig. 2*A*) (14, 15). A linear precursor (**5a**) for the first decagonal macrocycle was thus synthesized by a method developed for materials applications (16), and after conversion to **6a** via borylation (17), dimerization via Ni-mediated Yamamoto coupling was performed to synthesize the decagonal macrocycle (**7a**) having eight *t*-Bu and two boryl substituents. The macrocycle was furnished with two biphenyl units (**8a**), which were closed for a transannular bridge via **9a** to afford phenine polluxene **10a** comprising 14 trivalent vertices linked with 15 biaryl edges. The feasibility of the final ring-closing reaction was indeed expected by two relevant facts. First, we expected that the decagonal macrocycle should adopt a conformation similar to methano[10]annulene (18, 19), which should set the biphenyl rims at preferable positions to close the transannular, bascule bridge. Second, the biaryl linkages used as the edge of the minimal

Significance

Diamonds enchant people with their beauty, which has also been defined by mathematics. The existence of strong isotropy with maximal symmetry in carbon networks has been mathematically disclosed, which has led to a proposal of a diamond twin. Unlike tetrahedral vertices of the diamond, trigonal vertices of the diamond twin achieve strong isotropy, notably, with chirality. In the diamond twin, 14 trigonal vertices are connected by 15 edges to form a minimal cage. Although the diamond-twin network indeed had a four-decade history in theory, it remained imaginary in reality due to its inevitable instability of the minimal cage. In this paper, the carbonaceous minimal cage of the diamond twin has been synthesized, which reveals unique structural features including helical chirality.

Author contributions: K.I. and H.I. designed research; T.M.F., T.K., K.I., and H.I. performed research; T.M.F., T.K., K.I., and H.I. analyzed data; and T.M.F. and H.I. wrote the paper.

The authors declare no competing interest.

This article is a PNAS Direct Submission.

[1]To whom correspondence may be addressed. Email: kikemoto@chem.s.u-tokyo.ac.jp or isobe@chem.s.u-tokyo.ac.jp.

This article contains supporting information online at http://www.pnas.org/lookup/suppl/doi:10.1073/pnas.2120160119/-/DCSupplemental.

Published February 7, 2022.

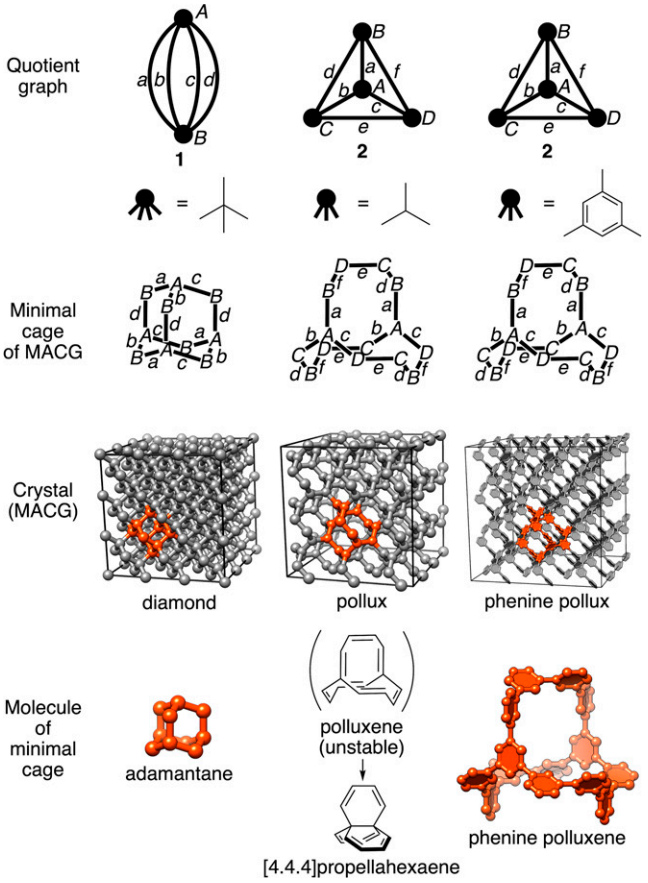

Fig. 1. Strongly isotropic networks revealed by topological crystallography. Diamonds and polluxes were found to be strongly isotropic MACGs that were derived from corresponding quotient graphs with tetravalent and trivalent vertices, respectively. Adopting fundamental vertices and edges, MACGs gave rise to minimal cages of adamantane and polluxene as segmental molecules. Polluxene composed of sp^2-carbon atoms was not located as a stable molecule by DFT calculations at the B3LYP/6-31G(d,p) level and collapsed into a ring-closed [4.4.4]propellahexaene molecule. Replacing sp^2-carbon atoms of polluxene with phenine resulted in the phenine polluxene that was conceived and synthesized in this work.

cage can tolerate bond rotations and, unlike highly conjugated bonds between sp^2-carbon vertices, can adopt the twisted orientations required by the mathematical demand to fulfill the polluxene network (5). The synthetic route was versatile enough to tolerate different substituents to expand the phenine network, and phenine-expanded polluxene **10b** was likewise synthesized. The effects of phenine expansion were preliminarily examined by absorption spectra. Thus, the absorption onset of **10a** with an 84π-system appeared at 313 nm, which was redshifted to 326 nm with **10b** having a larger 156π-system (Fig. 2*B*).

Crystal Structure and Chirality. The synthesis of the minimal cage in the form of phenine polluxene allowed us to clarify the uniqueness of the chirality of the fused decagonal cage via a series of structural analyses. We first clarified the molecular structure of **10a** by single-crystal X-ray crystallography. Although there were potentially many possible isomeric structures (see *Stereoisomerism*), phenine polluxene existed as a pair of enantiomers in the crystal. The enantiomer pair of **10a** emerged from the chirality due to the D_3 point symmetry, which was detailed by scrutinizing the molecular structure (Fig. 3*A*). Thus, a pair of bridgehead phenine panels were triply connected by looped phenine bridges to form a nanometer-sized cage. Depicting phenine panels of the crystal structure with round disks allowed us to clarify the presence of symmetry operations, and one C_3 axis and three C_2 axes were found to render the overall structure of the D_3 point symmetry. When the molecule was viewed along the C_3 axis that penetrated phenine vertices, the helicity associated with D_3-**10a** became evident. For instance, with the enantiomer shown in Fig. 3*A*, all three bridges formed right-handed screws around the C_3 axis (Fig. 3*A*), and its mirror-image isomer possessed screwed bridges in an opposite sense (see Fig. 3*B*). Thus, two enantiomers can be discriminated as a mirror-image pair by considering the helical sense of the screwed bridges around the C_3 axis; by taking into account the helicity nomenclatures of IUPAC (20), we propose to designate the stereoisomer with right-handed screwed bridges as the (*P*)-isomer. With this designation, the crystal packing containing (*P*)- and (*M*)-enantiomers of **10a** can be discriminated and designated in a clear manner, as shown in Fig. 3*B* (21). Notably, as the C_3/C_2 axes of polluxene were inherited from the infinite pollux network in the $I4_132$ space group (see Fig. 1) (6, 7, 22), the helicity nomenclature for polluxene can be directly applied to pollux. Thus, we may define the nomenclature in general as follows. When viewed along the C_3 symmetry axis penetrating a trivalent vertex, pollux/polluxene possesses three bridges that connect one vertex on a front side to another vertex on a back side. When the bridges are screwed to form right-handed helices, pollux/polluxene is designated (*P*), whereas those with left-handed helices are designated (*M*).

Stereoisomerism. The stereoisomerism of the fused decagonal cages was further investigated in detail with the aid of combinatorial enumerations based on group theory. In general, enumeration of stereoisomers is the most fundamental and important step to get a whole picture of the stereoisomerism, and due to complicated topologies of cyclic systems, the structural mathematics is indispensable (13, 23). The stereoisomerism of phenine polluxene is complicated due to its cyclic and fused structure comprising 14 vertices connected with 15 edges. The edges were composed of twisted biaryl bonds that intrinsically possessed chirality axes. As a result, 2^{15} (= 32,768) redundant combinations of atropisomeric bonds emerge in total, which further gives rise to the unique cycloisomerism of a cage system (13, 24). To further elucidate the isomerism, we applied a combinatorial enumeration method that was derived from Pólya's theorem (25, 26). Thus, **10a** with D_3 point symmetry possesses a nonredundant set of subgroup (SSG) of $\{C_1, C_2, C_3, D_3\}$, and by taking into account the isomeric structures, we obtain a vector, $(2^{15}\ 2^8\ 2^5\ 2^3)$, as the SSG of phenine polluxene. Then, by applying the inverse of the table of marks for the D_3 point group to the SSG, we derive the total numbers of isomers as follows:

$$\begin{pmatrix} C_1 & C_2 & C_3 & D_3 \\ 2^{15} & 2^8 & 2^5 & 2^3 \end{pmatrix} \begin{pmatrix} \frac{1}{6} & 0 & 0 & 0 \\ -\frac{1}{2} & 1 & 0 & 0 \\ -\frac{1}{6} & 0 & \frac{1}{2} & 0 \\ \frac{1}{2} & -1 & -\frac{1}{2} & 1 \end{pmatrix} = \begin{pmatrix} C_1 & C_2 & C_3 & D_3 \\ 5332 & 248 & 12 & 8 \end{pmatrix}.$$

Thus, the total number of the nonredundant isomeric structures of **10a** reaches 5332 + 248 + 12+ 8 = 5,600.

Structural Fluctuations in Solution. Theoretical calculations further deepened our understanding of the chiral polluxene structure in solution. Among the 5,600 nonredundant structures, only 12 isomers (six enantiomer pairs) were found within an

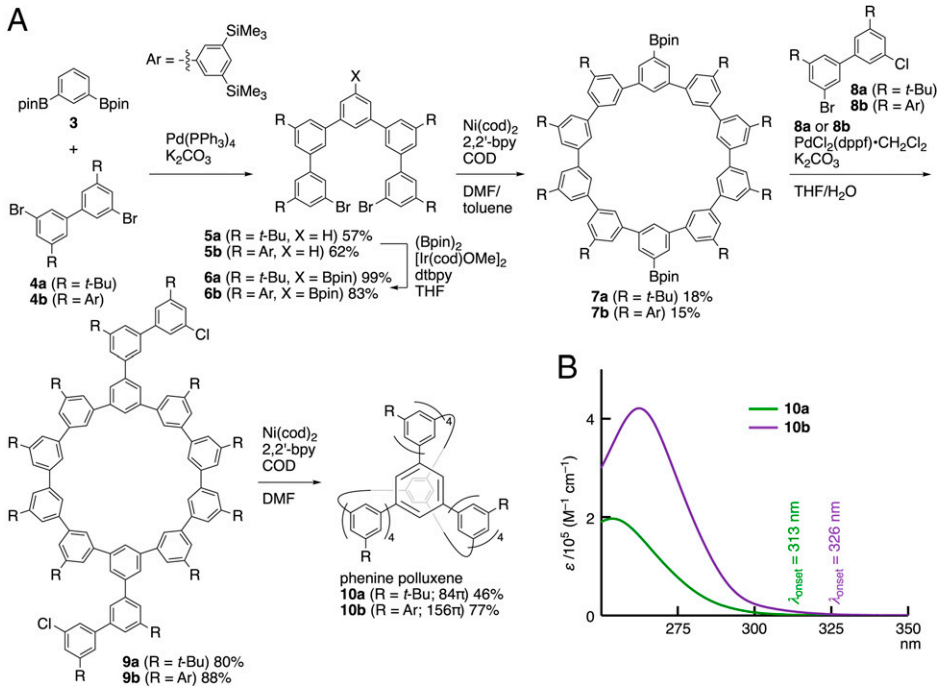

Fig. 2. Synthesis of phenine polluxene congeners. (*A*) Five-step synthesis of phenine polluxenes **10a** and **10b** with different substituents on the minimal cage. (*B*) Ultraviolet-visible (UV-vis) absorption spectra of **10a** and **10b** in chloroform at 25 °C.

energy range of +3 kcal · mol^{-1} from the global minimum via conformational search calculations (MM2* and $CHCl_3$) with a model having methyl substituents (*SI Appendix*) (27). The structure at the global minimum possessed D_3 point symmetry and reproduced the crystal structure of (*P*)/(*M*)-**10a** (see Fig. 3*B*). As expected from the *ortho*-substituent–free structure, the energy barrier for epimerization at the biaryl linkage was small. For instance, the energy barrier for the conversion of the global minimum structure to the second-stable structure was estimated as +3 kcal · mol^{-1} (*SI Appendix*), which suggested rapid interconversions of isomeric structures. Thus, the results suggested that when (*P*)- and (*M*)-**10a** racemate was dissolved in solution, rapid interconversions of conformers proceeded at ambient temperature, which resulted in the D_{3h} point symmetry of the average structure (Fig. 3*C*).

Chiral Polluxene. Taking advantage of the concise synthetic route, we then synthesized rigid chiral polluxenes and succeeded in chiral resolution. Considering that biaryl atropisomerism plays a determinant role in determining the helical chirality of polluxene, we installed an *ortho*-dimethylated linkage at one of the bridges for stereochemical rigidity. In the first preliminary attempt, dimethylated derivative **10c** was prepared (Fig. 4*A*), but the chiral resolution was not successful after examination of five different types of chiral columns. Realizing that the chiral cage should be concealed by radiated substituents, we then introduced two extra methoxy groups as auxiliary groups to facilitate chiral recognition. Consequently, we were delighted to find that a chiral column loaded with (*R*)-1-naphthylglycine succeeded in separating the two stereoisomers of $(+)_{300}$/$(-)_{300}$-**10d** (Fig. 4*B*) (28). Preliminary theoretical investigations on the rotational barrier indicated the presence of a high barrier of >30 kcal · mol^{-1}. The separated isomers gave mirror-image circular dichroism (CD) spectra (Fig. 4*C*), which confirmed the enantiomeric relationship between these two isomers. The conformational search calculations of **10d** with methyl substituents located a pair of enantiomers as the global minimum (Fig. 4*D*), which should exist as the most abundant structures in solution (~50% population of Boltzmann distributions). The conformational analyses also suggested that both the dominant structure and the Boltzmann-weighted average structure possess single-sense helices around the pseudo C_3 axis. Thus, (*S*)-biaryl linkages of **10d** resulted in right/right/right screwed bridges both in the average and global minimum structures, and hence the structure should best be represented as (*P*)-**10d** (*SI Appendix*). We then performed time-dependent (TD) DFT calculations to simulate a theoretical CD spectrum from the global minimum structure of (*P*)-**10d**; as shown in Fig. 4*C*, the spectrum matched well with that of $(+)_{300}$-**10d**. Further confirmation of X-ray crystallography should be performed in the future to confirm the configurational assignment of the helicity. Nonetheless, a pair of enantiomers was separated with the rigid chiral polluxene derivative to afford two stereoisomers with mirror-image CD spectra.

Conclusions

The trivalent planar units of phenine were assembled as vertices of fused decagonal cycles to form a minimal cage of the diamond twin, pollux, which added a unique example to modern repertoire of molecular cages (14, 15, 29–31). Although pollux has been an imaginary, long-sought entity of theoretical interest (3, 6), the synthesis of the minimal cage showed that it now becomes a reachable, synthetic target by adopting stable trivalent units such as phenine. The nanometer-sized cage, named phenine polluxene, revealed a unique molecular structure both by experiments and in theory to demonstrate the presence of a chiral network. The chirality of the pollux/polluxene networks originated from the helicity around the major C_3 axis, which should be discriminated by the triple helix made of three screwed bridges around the C_3 axis. Asymmetric syntheses and expansions of the phenine networks should be an intriguing target to be explored in the next stage for chiral carbon-rich materials.

Materials and Methods

Synthesis. Phenine polluxenes (**10a-d**) were synthesized by a common stepwise route combining multiple biaryl coupling reactions. Structures were identified

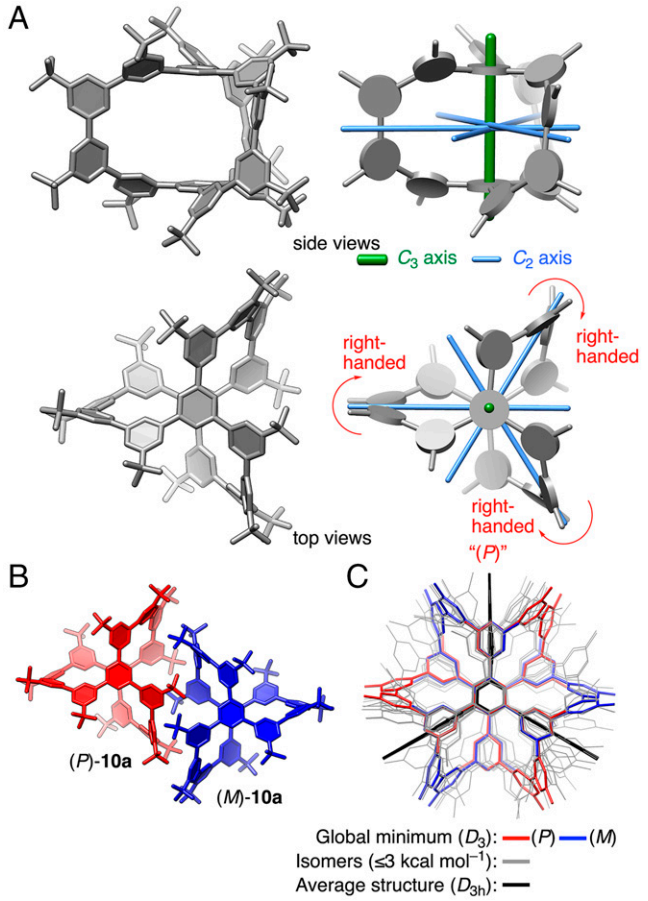

Fig. 3. Molecular structures of phenine polluxene. (*A*) Crystal structures of **10a**. In addition to the standard molecular models on the left, schematic representations with symmetry operations are shown on the right. Schematic representations were created by using the coordinates of the crystal structure and replacing phenine panels with disks. As a representative structure, one of the enantiomers is shown. (*B*) An enantiomer pair of **10a** in the crystal packing. (*C*) Theoretical structures obtained from the conformational search analyses of **10a** with methyl substituents. Two enantiomeric structures are shown in red/blue, and low-energy stereoisomeric structures are shown in gray. Within an energy window of 3 kcal · mol^{-1} from the global minimum, 12 isomeric structures were found. A Boltzmann-weighted average structure of the isomeric structure is shown in black.

by spectroscopic analyses with proofs of purity from high-performance liquid chromatography (HPLC) analyses. Chiral resolutions of **10d** were chromatographically achieved by using SUMICHIRAL OA-2500 columns. Further details of procedures and results are described in *SI Appendix*.

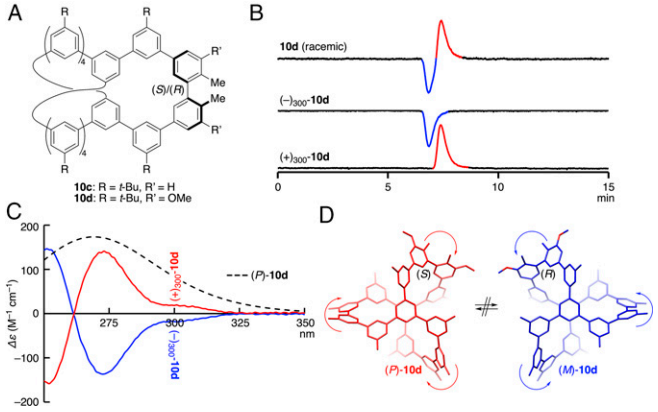

Fig. 4. Chiral resolution of polluxene. (*A*) Synthesized polluxene (**10c** and **10d**) with stereochemical rigidity. (*B*) Chiral resolution of **10d**. A chiral column loaded with (*R*)-1-naphthylglycine (SUMICHIRAL OA-2500, 4.6 × 250 mm) was used for the HPLC analyses (eluent = 0.5% 1-butanol/hexane; flow rate = 1.0 mL · min^{-1}, 40 °C). Stereoisomers were labeled with the CD sign at 300 nm. (*C*) CD spectra of enantiomers of **10d** in chloroform at 25 °C. A theoretical CD spectrum was obtained by TD DFT calculations at the B3LYP/6-31G(d,p)/PCM level with the (*P*)-isomer of **10d** having a methyl substituent. (*D*) An enantiomer pair found as the global minimum from the conformational search calculations of **10d** with methyl substituents (*SI Appendix*). The chromatographic chiral resolution of $(+)_{300}$- and $(-)_{300}$-enantiomers showed that these enantiomeric structures are not interconverted in solution at ambient temperature.

Crystallographic Analysis. A single crystal of phenine polluxene **10a** suitable for X-ray analysis was obtained by slow diffusion of methanol into chloroform solution at 25 °C. The diffraction analyses were carried out at −180 °C on a Rigaku XtaLAB P200 diffractometer equipped with a PILATUS200K area detector using multilayer mirror monochromated Cu-Kα radiation. From the diffraction data were obtained the structure by using the SHELXT program (32) for initial phase determination and the SHELXL program (33) for structural refinements of full-matrix least squares on F^2 on the Olex2 program (34). Further details of analyses are described in *SI Appendix*.

Theoretical Structural Analysis. Conformational search analyses of phenine polluxenes **10a** and **10d** were performed with MacroModel (35) to reveal structural fluctuations in solution. For the detailed energetics and spectral simulations, DFT calculations were performed with Gaussian 16 (36). Further details of calculations are described in *SI Appendix*.

Data Availability. Crystallographic data were deposited in the Cambridge Crystallographic Data Centre (CCDC 2112859). The data can be obtained free of charge from the CCDC via http://www.ccdc.cam.ac.uk/data_request/cif.

ACKNOWLEDGMENTS. We thank Prof. M. Kotani for stimulating discussion on the K_4 crystal in 2009 at Tohoku University and Dr. D. Yoshidome (Schrödinger) for generous guides of Maestro. T.M.F. thanks Japan Society for the Promotion of Science (JSPS) for a predoctoral fellowship. This study is partly supported by Grants-in-Aid for Scientific Research, KAKENHI (20H05672 and 20K15254).

1. R. C. Fort, P. V. R. Schleyer, Adamantane: Consequences of the diamondoid structure. *Chem. Rev.* **64**, 277–300 (1964).
2. J. E. Dahl, S. G. Liu, R. M. K. Carlson, Isolation and structure of higher diamondoids, nanometer-sized diamond molecules. *Science* **299**, 96–99 (2003).
3. T. Sunada, *Topological Crystallography: With a View Towards Discrete Geometric Analysis* (Springer, 2013).
4. M. Kotani, T. Sunada, Standard realizations of crystal lattices via harmonic maps. *Trans. Am. Math. Soc.* **353**, 1–20 (2001).
5. T. Sunada, Crystals that nature might miss creating. *Not. Am. Math. Soc.* **55**, 208–215 (2008).
6. M. V. Nikerov, D. A. Bochvar, I. V. Stankevich, Allotropic modifications of carbon. *J. Struct. Chem.* **23**, 150–152 (1982).
7. P. Davide *et al.*, In Samara Carbon Allotrope Database (SACADA), see references with a keyword of "Topology = srs." https://www.sacada.info/. Accessed 3 February 2022.
8. R. Hoffmann, A. A. Kabanov, A. A. Golov, D. M. Proserpio, *Homo citans* and carbon allotropes: For an ethics of citation. *Angew. Chem. Int. Ed. Engl.* **55**, 10962–10976 (2016).
9. M. Itoh *et al.*, New metallic carbon crystal. *Phys. Rev. Lett.* **102**, 055703 (2009).
10. Y. Yao *et al.*, Comment on "New metallic carbon crystal". *Phys. Rev. Lett.* **102**, 229601 (2009).
11. L. A. Paquette *et al.*, [4.4.4]Propellahexaene by triple Shapiro degradation. Structural and electronic properties of this maximally unsaturated hydrocarbon and consequences of O-methylation of its [4.4.4]propellatrienetrione precursors. *J. Org. Chem.* **55**, 1598–1611 (1990).
12. K. Ikemoto, H. Isobe, Geodesic phenine frameworks. *Bull. Chem. Soc. Jpn.* **94**, 281–294 (2021).
13. Z. Sun, T. Matsuno, H. Isobe, Stereoisomerism and structures of rigid cylindrical cycloarylenes. *Bull. Chem. Soc. Jpn.* **91**, 907–921 (2018).
14. E. Kayahara *et al.*, Synthesis and physical properties of a ball-like three-dimensional π-conjugated molecule. *Nat. Commun.* **4**, 2694 (2013).
15. K. Matsui, Y. Segawa, T. Namikawa, K. Kamada, K. Itami, Synthesis and properties of all-benzene carbon nanocages: A junction unit of branched carbon nanotubes. *Chem. Sci. (Camb.)* **4**, 84–88 (2013).
16. A. Yoshii *et al.*, Acyclic, linear oligo-*meta*-phenylenes as multipotent base materials for highly efficient single-layer organic light-emitting devices. *Chem. Asian J.* **15**, 2181–2186 (2020).
17. K. Ikemoto *et al.*, Modular synthesis of aromatic hydrocarbon macrocycles for simplified, single-layer organic light-emitting devices. *J. Org. Chem.* **81**, 662–666 (2016).
18. S. W. Slayden, J. F. Liebman, The energetics of aromatic hydrocarbons: An experimental thermochemical perspective. *Chem. Rev.* **101**, 1541–1566 (2001).

19. J. Y. Xue, K. Ikemoto, S. Sato, H. Isobe, Introduction of nitrogen atoms in [*n*]cyclo-*meta*-phenylenes via cross-coupling macrocyclization. *Chem. Lett.* **45**, 676–678 (2016).
20. In International Union of Pure and Applied Chemistry (IUPAC) Gold Book, see "helicity." https://goldbook.iupac.org/terms/view/H02763. Accessed 3 February 2022.
21. T. O. Yeates, S. B. H. Kent, Racemic protein crystallography. *Annu. Rev. Biophys.* **41**, 41–61 (2012).
22. M. I. Aroyo, Ed., *International Tables for Crystallography, Volume A* (Space-group Symmetry Series, Wiley, ed. 6, 2016).
23. Z. Sun *et al.*, Stereoisomerism, crystal structures, and dynamics of belt-shaped cyclonaphthylenes. *Proc. Natl. Acad. Sci. U.S.A.* **113**, 8109–8114 (2016).
24. E. L. Eliel, S. H. Wilen, Eds., *Stereochemistry of Organic Compounds* (Wiley, 1994).
25. S. Fujita, *Symmetry and Combinatorial Enumeration in Chemistry* (Springer-Verlag Berlin Heidelberg, 1991).
26. S. Fujita, Application of coset representations to the construction of symmetry adapted functions. *Theor. Chim. Acta* **78**, 45–63 (1990).
27. H. Isobe, H. Tokuyama, M. Sawamura, E. Nakamura, Synthetic and computational studies on symmetry-defined double cycloaddition of a new tris-annulating reagent to C_{60}. *J. Org. Chem.* **62**, 5034–5041 (1997).
28. N. Ôi, H. Kitahara, F. Aoki, N. Kisu, Direct separation of carboxylic acid enantiomers by high-performance liquid chromatography with amide and urea derivatives bonded to silica gel as chiral stationary phases. *J. Chromatogr. A* **689**, 195–201 (1995).
29. H. Sato, J. A. Bender, S. T. Roberts, M. J. Krische, Helical rod-like phenylene cages via ruthenium catalyzed diol-diene benzannulation: A cord of three strands. *J. Am. Chem. Soc.* **140**, 2455–2459 (2018).
30. N. Hayase, J. Nogami, Y. Shibata, K. Tanaka, Synthesis of a strained spherical carbon nanocage by regioselective alkyne cyclotrimerization. *Angew. Chem. Int. Ed. Engl.* **58**, 9439–9442 (2019).
31. L. J. Chen, H.-B. Yang, M. Shionoya, Chiral metallosupramolecular architectures. *Chem. Soc. Rev.* **46**, 2555–2576 (2017).
32. G. M. Sheldrick, SHELXT—Integrated space-group and crystal-structure determination. *Acta Crystallogr. A Found. Adv.* **71**, 3–8 (2015).
33. G. M. Sheldrick, Crystal structure refinement with SHELXL. *Acta Crystallogr. C Struct. Chem.* **71**, 3–8 (2015).
34. O. V. Dolomanov, L. J. Bourhis, R. J. Gildea, J. A. K. Howard, H. Puschmann, OLEX2: A complete structure solution, refinement and analysis program. *J. Appl. Cryst.* **42**, 339–341 (2009).
35. Release, *2021-3: MacroModel/Maestro* (Schrödinger, 2021).
36. M. J. Frisch *et al.*, *Gaussian 16 Revision A.03* (Gaussian, 2016).